PRAMANA
— journal of
physics

Vol. 57, Nos 2 & 3
Aug. & Sept. 2001
pp. 481–492

Superheavy nuclei – cold synthesis and structure

RAJ K GUPTA
Physics Department, Panjab University, Chandigarh 160 014, India

Abstract. The quantum mechanical fragmentation theory (QMFT), given for the cold synthesis of new and superheavy elements, is reviewed and the use of radioactive nuclear beams (RNB) and targets (RNT) is discussed. The QMFT is a complete theory of cold nuclear phenomena, namely, the cold fission, cold fusion and cluster radioactivity. Also, the structure calculations based on the axially deformed relativistic mean field (DRMF) approach are presented which predict new regions of spherical magicity, namely $Z = 120$ and $N = 172$ or 184, for superheavy nuclei. This result is discussed in the light of recent experiments reporting the cold synthesis of $Z = 118$ element.

Keywords. Superheavy nuclei; new magic numbers.

PACS No. 27.90.+b

1. Introduction

The cold synthesis of new and superheavy elements was proposed theoretically by us [1,2] sometime back in 1974–75 and a method was given for selecting out an optimum cold target-projectile combination. Cold compound systems were considered to be formed for *all* those target + projectile combinations that lie at the bottom of the *potential energy minima*, referred to as 'cold reaction valleys' or 'cold fusion reactions' [2–5]. This theory, called the quantum mechanical fragmentation theory (QMFT), was advanced as a unified approach both for fission (later, including the cluster radioactivity also) and heavy-ion collisions. The key result behind the cold fusion reaction valleys is the *shell closure effects* of one or both the reaction partners. The same refers to the decay products for (cold) fission and cluster radioactivity. The fission was also considered to be a cold phenomenon as early as in 1974 [6], prior to the 'Lohengrin' measurements of 1980 which established fission as a cold process. The new phenomenon of cluster radioactivity was predicted in 1980 [7] on the basis of the QMFT, once again prior to its observation in 1984. Thus, cold nuclear phenomena was proposed for the first time on the basis of the QMFT, and prior to experiments in each case. One of the aim of this talk is to review this theory and present some new calculations for reasons of planning for the future experiments, in particular the use of radioactive nuclear beams (RNB) and targets (RNT). It is shown that QMFT is a complete theory of cold phenomena of both the decay and fusion of nuclei. For further details, we refer to [8].

On the basis of the QMFT, four 'cold reaction valleys' were always found to exist with isotopes of Pb, Kr, Ca (or neighbouring nuclei) and the light nuclei, like C, N, O and Ne, as

one of the reaction partners always. These are in addition to the symmetric or nearly symmetric reaction partners which were found to be coldest (deepest potential energy minima), though *not* the best when this information on cold reaction valleys was optimized [2] by the requirements of smallest interaction barrier, largest interaction radius and non-necked (no saddle) nuclear shapes. Thus, the cases of 'cold', 'warm/ tepid' and 'hot' fusion reactions could be easily categorized here. Note that all these are the cases of minima in potential energy surfaces (PES) and hence are 'cold' with respect to 'hot' ones coming from 'outside' the minima in PES.

The interesting aspect of this study is that all the successful GSI and Dubna experiments made for synthesizing superheavy nuclei, upto $Z = 112$, used only Pb (or Bi for odd Z) targets. Very recently, an isotope of $Z = 118$ is also synthesized at Berkeley [9] by using ^{86}Kr beam on ^{208}Pb target. The reported cross section (2.2 pb) is rather large, compared to the limiting value (1 pb) so far measured for other cold fusion reactions, though a recent GSI re-confirmation of this experiment ended only in an upper limiting value of 0.5–1.0 pb. The fact that these are all cold fusion reactions was first confirmed in GSI experiments [10], where enhanced fusion cross sections were observed at lower excitation energies, or at incident energies below the barrier. Also, the ^{48}Ca beam was used successfully [11] in the early synthesis of $^{252}102$ isotope in its reaction with different Pb target nuclei. The compound nuclei formed in these reactions were with very low excitation energy (17–18 MeV) which proceeded to ground state with the emission of 1 to 2 neutrons. More recently, ^{48}Ca beam is used to produce rather *neutron-rich* $^{283}112$ and $^{289}114$ isotopes of $Z = 112$ and 114 elements in $3n$ emission reactions with ^{238}U and ^{244}Pu [12] targets, respectively. The resulting excitation energy is 33–35 MeV. This could be termed as 'tepid fusion' compared to 'cold' and 'hot' fusions having, respectively, the excitation energies around 20 and 50 MeV. The 'hot' fusion reactions are the $4n$ and $5n$ reactions using the light ion beams like ^{12}C, ^{18}O, ^{22}Ne and ^{34}S on heavy deformed actinides [12]. Compared to the 'cold fusion' reactions, the 'hot fusion' reactions are found to result in lower fusion cross sections. Thus, *all* the so far successful experiments use *exactly* the same reaction partners as were predicted and published for $Z = 100-116$ on the basis of the QMFT [2–5], more than two decades prior to the above experiments. The persistence of Pb valley was predicted again in 1997 [13] for $Z = 120$ and the use of RNB and RNT is advocated more recently [14].

The recent excitement in the study of superheavy elements stem from the very recent predictions of new magic numbers for both the protons and neutrons. In a spherical relativistic mean field calculation, Rutz *et al* [15] scanned a wide range of nuclei in superheavy region, using the various parameter sets, and predicted $Z = 120$ and $N = 172$ as the next spherical magic shells. On the other hand, based on a rather complete deformed relativistic mean field (DRMF) calculation, using the NL1 parameter set, we [16] predicted $Z = 120$ and $N = 184$ as the next possible magic numbers in the superheavy region. However, our more recent study [17] of the binding energies of $Z = 104-112$ nuclei point out to a better suitability of the NL3 parameter set, which when applied to $Z = 106-126$ nuclei, result in equally large shell gaps for $Z = 120$ at both $N = 172$ and 184. The second aim of this talk is to discuss some of these results, which point out that if the Berkeley measurements on cold fusion reaction ^{208}Pb(^{86}Kr, $1n$) [9] were correct, the large cross section for this reaction may mean pointing out to the magic or nearly magic character of $Z = 118$ and we may be approaching the centre of real island of stability around $Z = 120$.

2. Structure calculations – the relativistic mean field approach

In the relativistic mean field approach, we begin with the relativistic Lagrangian density for a nucleon-meson many-body system [15–17]:

$$\begin{aligned}\mathcal{L} = {} & \overline{\psi_i}\{i\gamma^\mu\partial_\mu - M\}\psi_i + \frac{1}{2}\partial^\mu\sigma\partial_\mu\sigma - \frac{1}{2}m_\sigma^2\sigma^2 - \frac{1}{3}g_2\sigma^3 - \frac{1}{4}g_3\sigma^4 - g_s\overline{\psi_i}\psi_i\sigma \\ & - \frac{1}{4}\Omega^{\mu\nu}\Omega_{\mu\nu} + \frac{1}{2}m_w^2V^\mu V_\mu + \frac{1}{4}C_3(V_\mu V^\mu)^2 - g_w\overline{\psi}_i\gamma^\mu\psi_iV_\mu - \frac{1}{4}\vec{B}^{\mu\nu}.\vec{B}_{\mu\nu} \\ & + \frac{1}{2}m_\rho^2\vec{\rho}^\mu.\vec{\rho}_\mu - g_\rho\overline{\psi}_i\gamma^\mu\vec{\tau}\psi_i.\vec{\rho^\mu} - \frac{1}{4}F^{\mu\nu}F_{\mu\nu} - e\overline{\psi}_i\gamma^\mu\frac{(1-\tau_{3i})}{2}\psi_iA_\mu, \end{aligned} \tag{1}$$

where, σ is the field for σ-meson, V_μ that of the ω-meson and $\vec{\rho}_\mu$ of the isovector ρ-meson. The electromagnetic field is denoted by A^μ and the Dirac spinors for the nucleons by ψ_i whose third component of isospin is denoted by τ_{3i}. Here g_s, g_w, g_ρ and $\frac{e^2}{4\pi}(=\frac{1}{137})$ are the coupling constants for σ, ω, ρ mesons and photon, respectively, and g_2 and g_3 and C_3 are the parameters for the nonlinear terms of σ and ω mesons. M is the mass of nucleon and m_σ, m_ω and m_ρ are the masses of the σ, ω and ρ mesons, respectively. The $\Omega^{\mu\nu}$, $\vec{B}^{\mu\nu}$ and $F^{\mu\nu}$ are the field tensors for V^μ, $\vec{\rho}^\mu$ and the photon fields, respectively. From the Lagrangian, we get field equations for mesons and nucleons. These equations are solved by expanding the upper and lower components of the Dirac spinors and the boson field wavefunctions with an initial deformation in a sufficiently large deformed harmonic oscillator basis. Then, the set of coupled equations are solved numerically by self-consistent iteration method.

The total binding energy of the system is the sum of $E_{\rm part}$ (the sum of the single-particle energies of nucleons), E_σ, E_ω, E_ρ, E_c, $E_{\rm pair}$ and E_{CM}, respectively, the contributions of the meson fields, the Coulomb field, the pairing energy and the non-relativistic approximation for center-of-mass energy correction ($E_{CM} = -\frac{3}{4}\,41A^{-\frac{1}{3}}$). The effects of pairing interaction are added in the BCS formalism, with constant pairing gaps.

Figure 1 gives our calculated proton single-particle energies for $Z = 106-126$, $A = 269-309$ nuclei (in steps of α-nuclei), using the NL3 parameter set. We notice that the shell gap at $Z = 120$ is always larger than the $Z = 114$ gap, atleast upto $Z = 120$ nucleus. Another strong shell gap at $Z = 138$ for $Z > 114$ nuclei and at $Z = 124$ for $Z > 120$ nuclei appear, which have not yet assumed much importance. Thus, the shell gap at $Z = 120$ is though largest for the $Z = 120$ nucleus, as expected due to the self-consistent nature of these calculations, it is most predominant for all superheavy nuclei. Similarly, the neutron single-particle energies show that the shell gap at $N = 172$ competes with the one at $N = 184$, and that the next higher shell gaps at $N = 198$, 228 and 258 could not be ignored. Also, a shell gap at $N = 164$ is equally predominant.

A more interesting result of this calculation (figure 2) is the prediction of a broad region of sphericity for $Z = 116 \pm 4$ nuclei, flanked by prolate shaped nuclei for $Z < 112$ and oblate shapes for $Z > 120$ nuclei. The predictive power of these calculations is evident from the binding energy calculations in figure 3, the only measured quantity at present for superheavy nuclei. We notice that the NL3 parameter set gives the best results, within only ~ 5 MeV of experiments for all the observed cases.

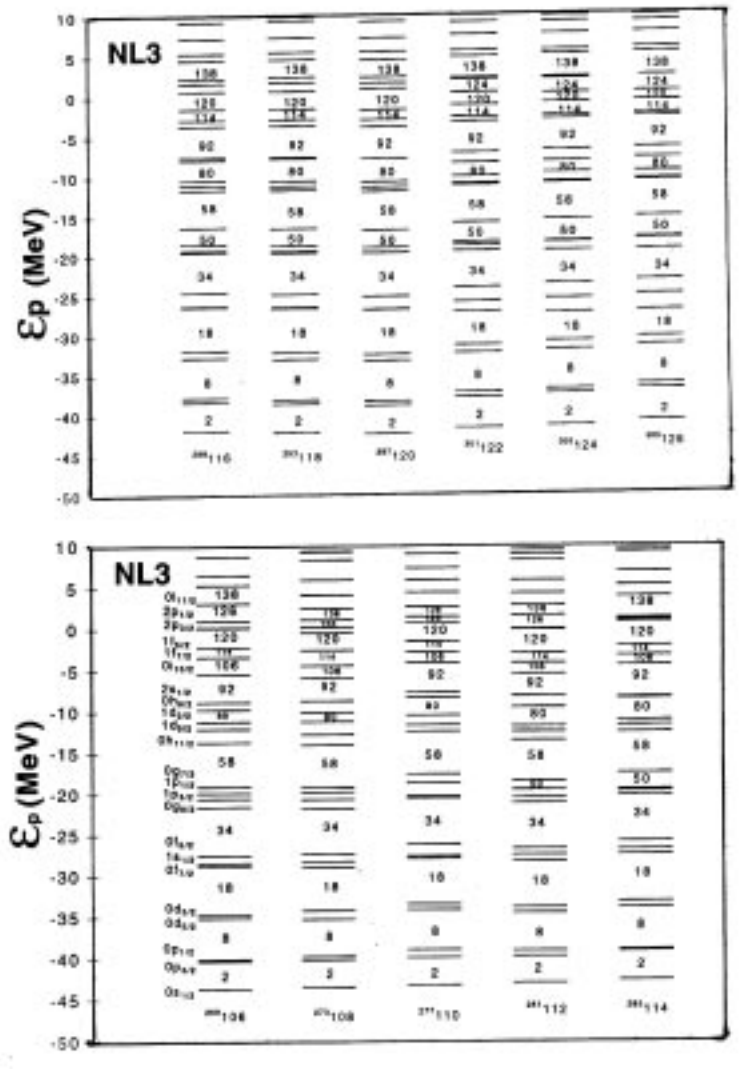

Figure 1. The proton single-particle energy spectra for $Z = 106-126$ nuclei, using NL3 parameter set [17].

3. Quantum mechanical fragmentation theory (QMFT)

The QMFT is a dynamical theory of all the three cold processes of fission, cluster radioactivity and fusion (or, in general, heavy-ion collisions), worked out in terms of the coordinates of mass (and charge) asymmetry $\eta = (A_1 - A_2)/A$ (and $\eta_Z = (Z_1 - Z_2)/Z$), the relative separation $\vec{R}$, the deformations β_1 and β_2 of two nuclei (or, in general, fragments), and the neck parameter ϵ [6,18]. For heavy-ion collisions, the time-dependent Schrödinger equation in η (taking η and η_Z motions as weakly coupled),

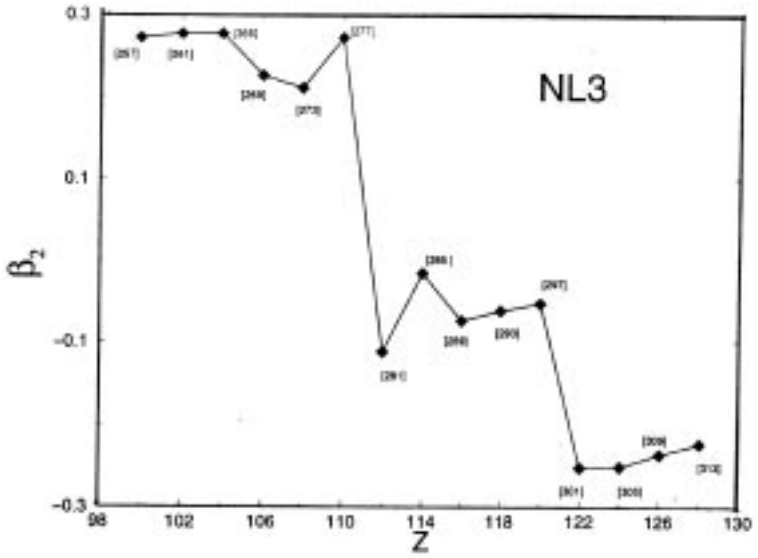

Figure 2. Deformation parameter β, using NL3 parameters [17].

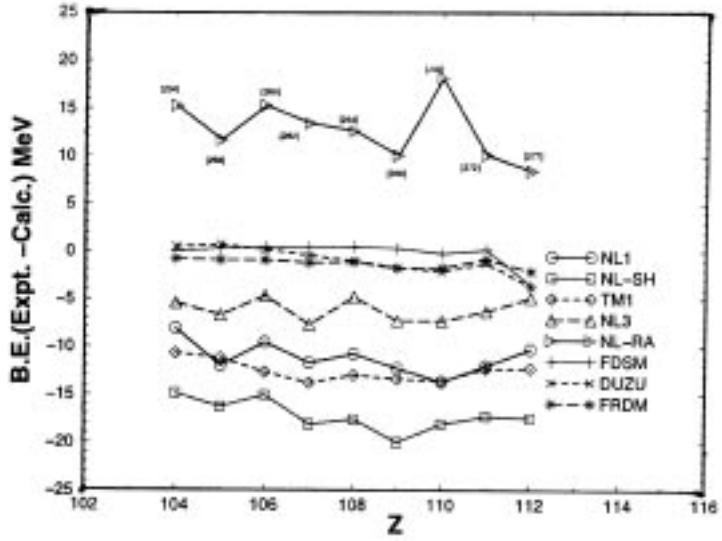

Figure 3. The differences in experimental and calculated ground state binding energies, using DRMF and other models [17].

$$H\Psi(\eta,t) = i\hbar\frac{\partial}{\partial t}\Psi(\eta,t), \tag{2}$$

is solved for $R(t)$ treated classically and the other coordinates β_1, β_2 and ϵ fixed by minimizing the collective potential in these coordinates. Equation (2) is solved for a number

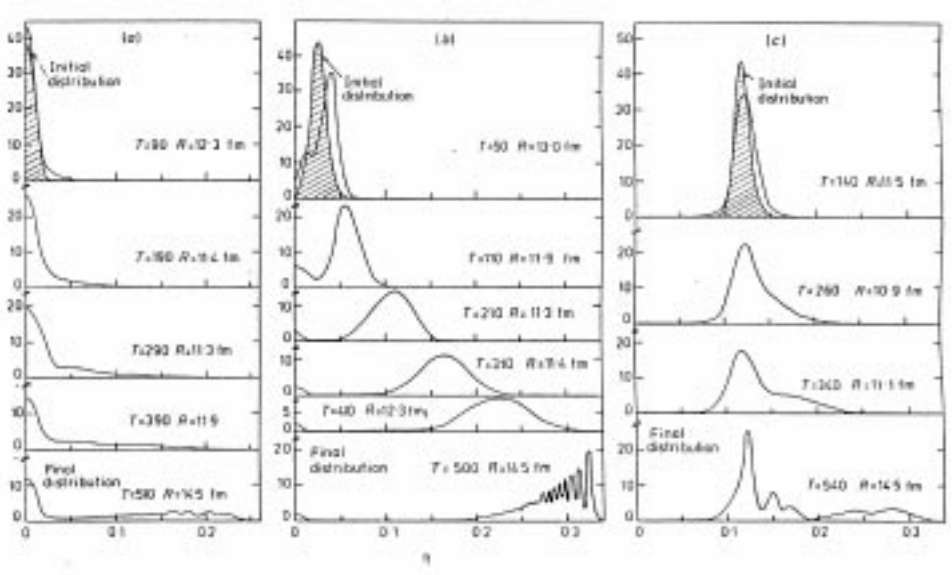

Figure 4. Time evolution of the mass fragmentation process at $E_{cm} = 820$ MeV, $L = 200\hbar$ and impact parameter $b = 2.9$ fm, for (**a**) ^{238}U + ^{238}U (a shallow minimum), (**b**) ^{232}Th + ^{244}Pu (outside minimum) and (**c**) ^{210}Pb + ^{266}No (a minimum), forming the same compound system [18].

of heavy systems [18] and figure 4 illustrates our results for different target + projectile combinations forming the same compound system. It is evident that for target + projectile combinations coming from *outside* the potential energy minima, a few nucleon to a large mass transfer occurs, whereas the same is zero for target + projectile referring to potential energy minima. This means that *for cold reaction partners, the two nuclei stick together and form a deformed compound system*. A few nucleon transfer may, however, occur depending on whether a 'conditional' saddle (see figure 7) exists or not. Since the solution of eq. (2) is very much computer-time consuming, in the following we look for simplifications based on calculated quantities.

The potentials $V(R,\eta)$ and $V(R,\eta_Z)$, calculated within Strutinsky method ($V = V_{\rm LDM} + \delta U$, liquid drop energy plus shell effects calculated by using the asymmetric two-center shell model (ATCSM)), show that the motions in both η and η_Z are much faster than the R-motion. This means that both the potentials $V(R,\eta)$ and $V(R,\eta_Z)$ are nearly independent of R-coordinate (see e.g figure 12 in [5]) and hence R can be taken as a time-independent parameter. This reduces the time-dependent Schrödinger eq. (2) to a stationary Schrödinger equation in η,

$$\left\{-\frac{\hbar^2}{2\sqrt{B_{\eta\eta}}}\frac{\partial}{\partial\eta}\frac{1}{\sqrt{B\eta\eta}}\frac{\partial}{\partial\eta}+V_R(\eta)\right\}\Psi_R^{(\nu)}(\eta)=E_R^{(\nu)}\Psi_R^{(\nu)}(\eta), \tag{3}$$

where $B_{\eta\eta}$ are the cranking masses, calculated consistently by using ATCSM, and R is fixed at the post-saddle point. This choice of R-value is justified by many good fits to both

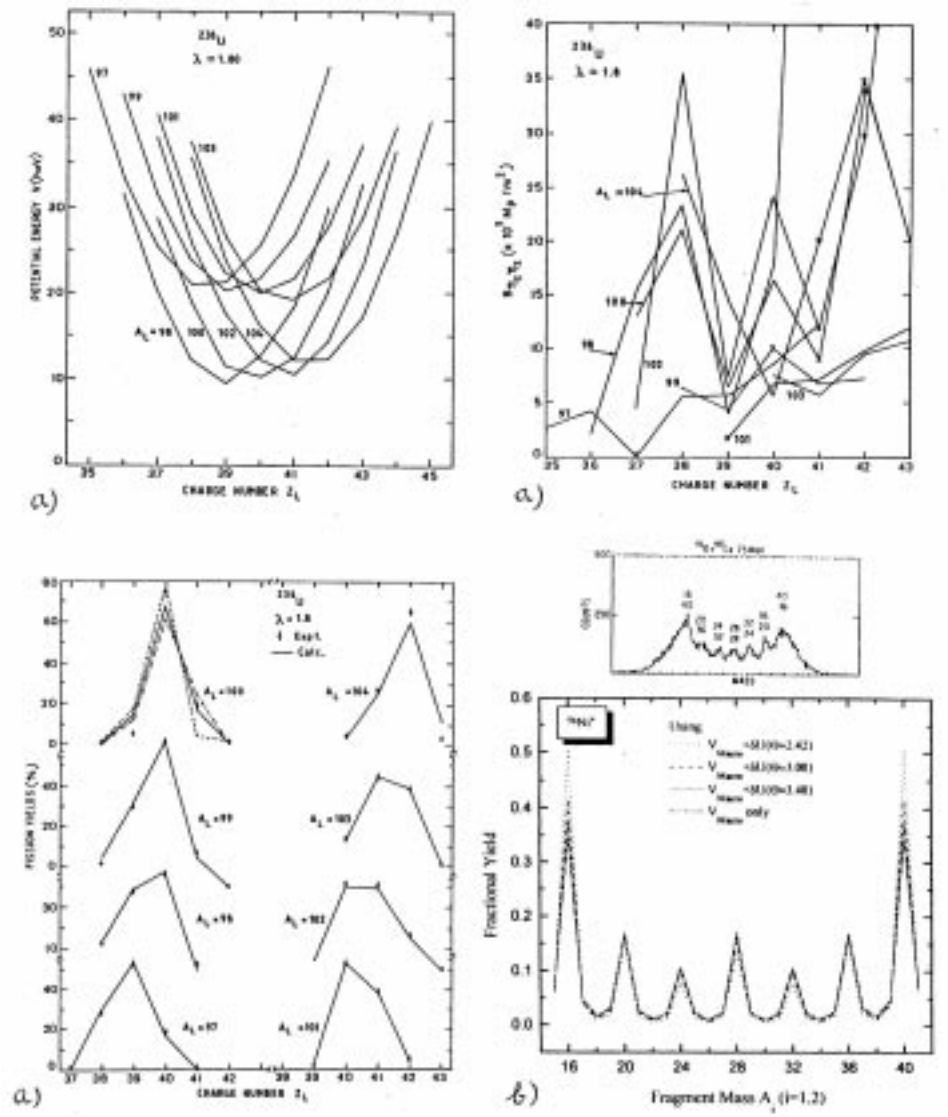

Figure 5. (**a**) $V(\eta)$, $B_{\eta\eta}$ and charge distribution yields compared with experiments for fission of ^{236}U (based on [21]). (**b**) Calculated and experimental fractional yields for the decay of excited ^{56}Ni* [22].

fission and heavy-ion collision data, illustrated in figure 5, and by an explicit, analytical solution of time-dependent Schrödinger equation in η_Z [19]. An interesting result of these calculations (figure 5) is that the yields ($\propto|\ \Psi(\eta)|^2$ or $|\ \Psi(\eta_Z)|^2$) are nearly insensitive to the detailed structure of the cranking masses. In other words, the static potential $V(\eta)$ or $V(\eta_Z)$ contain all the important information of a fissioning or colliding system. Since

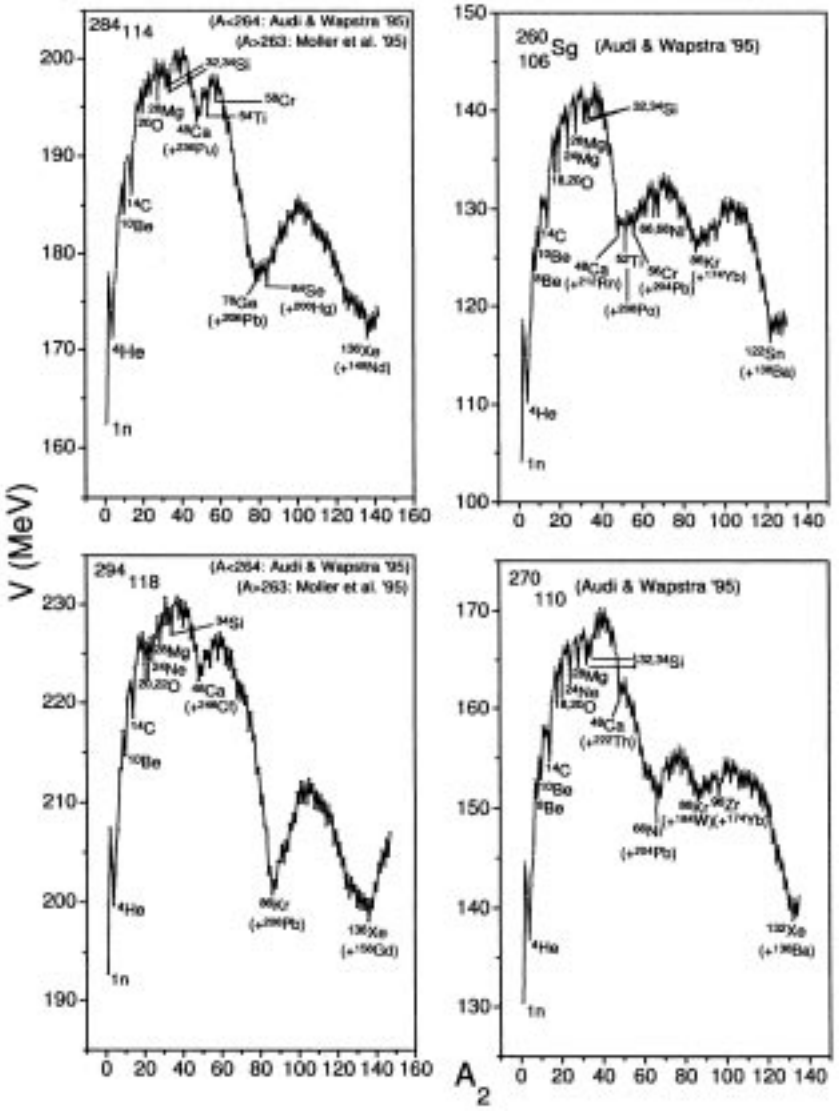

Figure 6. Potential energy surfaces, calculated at $R = R_c$, for various compound systems with $Z = 106-118$ refs [2–5,14].

these potentials are nearly independent of the choice of R-value, we have calculated them at some critical distance R_c where the two nuclei come in close contact with each other. Then, the potential $V(\eta, \eta_Z)$ is given simply as

$$V(R_c, \eta, \eta_Z) = \frac{Z_1 Z_2 e^2}{R_c} - \sum_{i=1}^{2} B(A_i, Z_i, \beta_i) + V_P \tag{4}$$

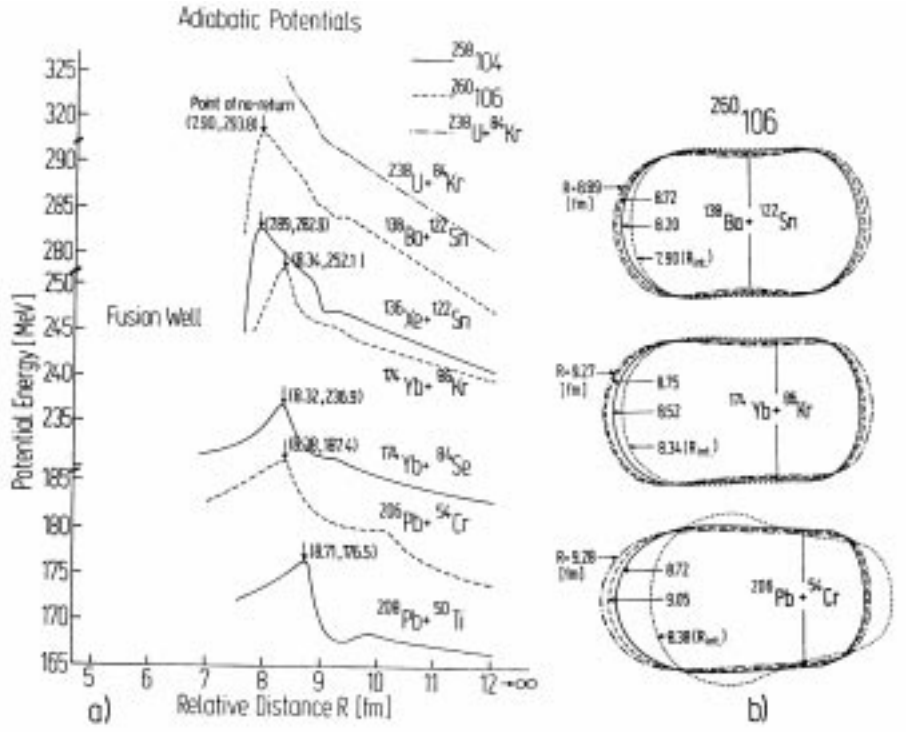

Figure 7. (**a**) Interaction potentials $V(R)$ for different target-projectile combinations, and (**b**) the corresponding two-centre nuclear shapes [2].

with B_i as the ground-state binding energies of two nuclei and charges Z_1 and Z_2 fixed by minimizing the potential in η_Z, which fixes β_i automatically. The proximity potential $V_{\rm P}$ is added for accounting the additional attraction between nuclear surfaces which changes only the relative excitations, and hence relative yields, but not the positions of the minima in PES [20]. The positions of the minima are due to shell effects only.

Figure 6 gives the calculated PES based on eq. (4). Two results are evident: (i) the minima correspond to atleast one closed shell nucleus, like ^{208}Pb, ^{86}Kr and/or ^{48}Ca, (ii) the ^{208}Pb or ^{86}Kr minimum is deeper than the ^{48}Ca minimum, which means that the reactions involving Pb nuclei are with lower excitation energies. The use of ^{86}Kr beam was also suggested in our very first publications on QMFT [2–5] and was stressed again recently very explicitly [13,23]. Specifically, ^{94}Sr + ^{208}Pb was predicted as the best cold fusion reaction for producing ^{302}120 nucleus [13]. Note that ^{94}Sr is a deformed nucleus and the use of spherical $^{88}_{38}\mathrm{Sr}_{50}$ for a lighter isotope of $Z = 120$ or $^{86}_{36}\mathrm{Kr}_{50}$ for $Z = 118$ element should be of further advantage in a cold fusion reaction, as shown explicitly in figure 6.

Table 1 lists all the possible target + projectile combinations, referring to minima in PES, other than the super-asymmetric combinations involving light nuclei. Some neighbouring target+projectile combinations are also included, since they could also be of interest from the point of view of experiments. We notice in table 1 that most of the light nuclei and some heavier nuclei are radioactive nuclei. This means that use of both the radioactive

Table 1. The targets and projectiles for cold fusion reactions, referring to minima in $V(R_c, \eta, \eta_Z)$, with neighbouring nuclei marked (*), the radioactive ones put in boxes, ones with half-life in ms marked (†) and so far unknown marked (?) [14].

Nucleus	η	Projectile	Target	Nucleus	η	Projectile	Target
$^{258}_{104}$Rf	0.627	^{48}Ca	$\boxed{^{210}\text{Po}}$	$^{284}114$	0.661	^{48}Ca	$\boxed{^{236}\text{Pu}}$
	0.596	$\boxed{^{52}\text{Ti}}$	^{206}Pb		0.450	$\boxed{^{78}\text{Ge}}$	^{206}Pb
	0.348	$\boxed{^{84}\text{Se}}$	^{174}Yb		0.408	$\boxed{^{84}\text{Se}}$	^{200}Hg
	0.318	$\boxed{^{88}\text{Kr}}$	^{170}Er(*)		0.394	^{86}Kr	^{198}Pt
	0.038	^{124}Sn	^{134}Xe		0.042	^{136}Xe	^{148}Nd
$^{260}_{106}$Sg	0.630	^{48}Ca	$\boxed{^{212}\text{Rn}}$	$^{288}114$	0.652	$\boxed{^{50}\text{Ca}}$	$\boxed{^{238}\text{Pu}}$
	0.600	$\boxed{^{52}\text{Ti}}$	$\boxed{^{208}\text{Po}}$		0.444	$\boxed{^{80}\text{Ge}}$	^{208}Pb
	0.569	$\boxed{^{56}\text{Cr}}$	^{204}Pb		0.416	$\boxed{^{84}\text{Se}}$	^{204}Hg(*)
	0.338	^{86}Kr	^{174}Yb		0.069	$\boxed{^{134}\text{Te}}$	^{154}Sm
	0.061	^{122}Sn	^{138}Ba				
$^{270}_{108}$Hs	0.629	$\boxed{^{50}\text{Ca}}$	$\boxed{^{220}\text{Ra}}$(†)	$^{290}114$	0.655	$\boxed{^{50}\text{Ca}}$	$\boxed{^{240}\text{Pu}}$
	0.540	$\boxed{^{62}\text{Fe}}$	^{208}Pb		0.434	$\boxed{^{82}\text{Ge}}$	^{208}Pb
	0.496	$\boxed{^{68}\text{Ni}}$	^{202}Hg(*)		0.420	$\boxed{^{84}\text{Se}}$	$\boxed{^{206}\text{Hg}}$(*)
	0.377	$\boxed{^{84}\text{Se}}$	^{186}W		0.075	$\boxed{^{134}\text{Te}}$	$\boxed{^{156}\text{Sm}}$
	0.007	^{134}Xe	^{136}Xe				
$^{272}_{108}$Hs	0.632	$\boxed{^{50}\text{Ca}}$	$\boxed{^{222}\text{Ra}}$	$^{294}114$	0.659	$\boxed{^{50}\text{Ca}}$	$\boxed{^{244}\text{Pu}}$
	0.618	$\boxed{^{52}\text{Ti}}$	$\boxed{^{220}\text{Rn}}$(*)		0.428	$\boxed{^{84}\text{Ge}}$(†)	$\boxed{^{210}\text{Pb}}$(*)
	0.529	$\boxed{^{64}\text{Fe}}$	^{208}Pb		0.401	$\boxed{^{88}\text{Se}}$	$\boxed{^{206}\text{Hg}}$
	0.382	$\boxed{^{84}\text{Se}}$	$\boxed{^{188}\text{W}}$		0.306	$\boxed{^{102}\text{Zr}}$	^{192}W(?)
	0.309	$\boxed{^{94}\text{Sr}}$	$\boxed{^{178}\text{Yb}}$		0.102	$\boxed{^{132}\text{Sn}}$	$\boxed{^{162}\text{Gd}}$
	0.0	^{136}Xe	^{136}Xe				
$^{270}110$	0.644	^{48}Ca	$\boxed{^{222}\text{Th}}$(†)	$^{290}116$	0.668	^{48}Ca	$\boxed{^{242}\text{Cm}}$
	0.511	$\boxed{^{66}\text{Ni}}$	^{204}Pb		0.655	$\boxed{^{50}\text{Ca}}$	$\boxed{^{240}\text{Cm}}$
	0.362	^{86}Kr	^{184}W		0.420	$\boxed{^{84}\text{Se}}$	^{206}Pb
	0.289	^{96}Zr	^{174}Yb		0.062	^{136}Xe	^{154}Sm
	0.022	^{132}Xe	^{138}Ba				
$^{278}112$	0.654	^{48}Ca	$\boxed{^{230}\text{U}}$	$^{294}118$	0.673	^{48}Ca	$\boxed{^{246}\text{Cf}}$
	0.482	$\boxed{^{72}\text{Zn}}$	^{206}Pb		0.414	^{86}Kr	^{208}Pb
	0.439	$\boxed{^{78}\text{Ge}}$	^{200}Hg		0.074	^{136}Xe	^{158}Gd
	0.395	$\boxed{^{84}\text{Se}}$	^{194}Pt				
	0.0	^{138}Ba	$\boxed{^{140}\text{Ba}}$				
$^{286}112$	0.650	$\boxed{^{50}\text{Ca}}$	$\boxed{^{236}\text{U}}$	$^{302}120$	0.631	$\boxed{^{50}\text{Ca}}$	$\boxed{^{252}\text{Fm}}$
	0.455	$\boxed{^{78}\text{Zn}}$	^{208}Pb		0.356	$\boxed{^{94}\text{Sr}}$	^{208}Pb
	0.427	$\boxed{^{82}\text{Ge}}$	^{204}Hg		0.093	^{136}Xe	$\boxed{^{166}\text{Dy}}$
	0.062	$\boxed{^{134}\text{Te}}$	$\boxed{^{152}\text{Nd}}$				

beams and radioactive targets is very much suggested in our study of cold synthesis of new heavy and superheavy elements.

The above information of more than one 'cold reaction' valleys is further optimized by adding the requirements of smallest interaction barrier, largest interaction radius and non-necked (no saddle) nuclear shapes [2], as is illustrated in figure 7. The barrier height is lowest for the combination with ^{208}Pb but the barrier position has the largest value. The nuclear shapes are also non-necked only for the combination with ^{208}Pb. Like necked-in shapes are known [6] to witness the preformation of fission fragments, non-necked shapes are the signatures of cold fusion of two nuclei. Also, a kind of 'conditional saddle' is seen to be formed in some cases, which is a signature of the deep inelastic collisions component.

4. Summary

Summarizing, we have shown that the recent experimental discovery of the elements $Z = 110-112$ and 118 using the cold reactions with ^{208}Pb targets and that of $Z = 114$ using tepid reaction with ^{48}Ca beam were already predicted theoretically by Gupta *et al* [2–5] in 1976–77 on the basis of quantum mechanical fragmentation theory. Interesting enough, the use of radioactive beams (and targets) is shown to be of preferred choice for many superheavy nuclei, in particular the neutron-rich isotopes. Note that the QMFT, being a quantum mechanical theory, does not preclude other fusion reactions, but predict them to be less probable. Furthermore, the dynamical calculations support the hypothesis of cold fusion for target + projectile combinations referring to potential energy minima and show a few nucleon to large mass transfer process for target-projectile combinations coming from outside the potential energy minima.

References

[1] H J Fink, W Greiner, R K Gupta, S Liran, H J Maruhn, W Scheid and O Zohni, *Proc. Int. Conf. on Reactions between Complex Nuclei*, Nashville, June 1974, (North Holland) p. 21

[2] A Săndulescu, R K Gupta, W Scheid and W Greiner, *Phys. Lett.* **B60**, 225 (1976)
R K Gupta, A Săndulescu and W Greiner, *Phys. Lett.* **B67**, 257 (1977)

[3] R K Gupta, C Pârvulescu, A Săndulescu and W Greiner, *Z. Physik* **A283**, 217 (1977)

[4] R K Gupta, A Săndulescu and W Greiner, *Z. Naturforsch* **A32**, 704 (1977)

[5] R K Gupta, *Sov. J. Part. Nucl.* **8**, 289 (1977)

[6] R K Gupta, W Scheid and W Greiner, *Phys. Rev. Lett.* **35**, 353 (1975)
J Maruhn and W Greiner, *Phys. Rev. Lett.* **32**, 548 (1974)

[7] A Săndulescu, D N Poenaru and W Greiner, *Sov. J. Part. Nucl.* **11**, 528 (1980)

[8] *Heavy elements and related new phenomena* edited by W Greiner and R K Gupta (World Sci. Publications, 1999) vols I & II

[9] V Ninov, K E Gregorich, W Loveland, A Ghiorso, D C Hoffman, D M Lee, H Nitsche, W J Swiatecki, U W Kirbach, C A Laue, J L Adams, J B Patin, D A Shaughnessy, D A Strellis and P A Wilk, *Phys. Rev. Lett.* **83**, 1104 (1999)

[10] S Hofmann, V Ninov, F P Hessberger, P Armbruster, H Folger, G Münzenberg, H J Schött, A G Popeko, A V Yeremin, A N Andreyev, S Saro, R Janik and M Leino, *Z. Phys.* **A350**, 277, 281 (1995); **354**, 229 (1996)

[11] G N Flerov, Yu Ts Oganessian, A A Pleve, N V Pronin and Yu P Tretyakov, Preprint JINR, D7-9555, Dubna 1976

[12] Yu A Lazarev, Yu V Lobanov, Yu Ts Oganessian, V K Utyonkov, F Sh Abdullin, G V Buklanov, B N Gikal, S Iliev, A N Mezentsev, A N Polyakov, I M Sedykh, I V Shirovsky, V G Subbotin, A M Sukhov, Yu S Tsyganov, V E Zhuchko, R W Lougheed, K J Moody, J F Wild, E K Hulet and J H McQuaid, *Phys. Rev. Lett.* **73**, 624 (1994)
[13] R K Gupta, G Münzenberg and W Greiner, *J. Phys. G: Nucl. Part. Phys.* **23**, L13 (1997)
[14] R K Gupta, M Balasubramaniam, G Münzenberg, W Greiner and W Scheid, *J. Phys. G: Nucl. Part. Phys.* **27**, 867 (2001)
[15] K Rutz, M Bender, T Bürvenich, T Schilling, P-G Reinhard, J A Maruhn and W Greiner, *Phys. Rev.* **C56**, 238 (1997)
[16] S K Patra, R K Gupta and W Greiner, *Mod. Phys. Lett.* **A12**, 1727 (1997)
[17] S K Patra, W Greiner and R K Gupta, *J. Phys. G: Nucl. Part. Phys.* **26**, L65 (2000)
[18] R K Gupta, *Phys. Rev.* **C21**, 1278 (1980)
S Yamaji, K H Ziegenhain, H J Fink, W Greiner and W Scheid, *J. Phys.* **G3**, 1283 (1977)
[19] D R Saroha, R Aroumougame and R K Gupta, *Phys. Rev.* **C27**, 2720 (1983)
[20] N Malhotra, R Aroumougame, D R Saroha and R K Gupta, *Phys. Rev.* **C33**, 156 (1986)
[21] D R Saroha and R K Gupta, *Phys. Rev.* **C29**, 1101 (1984)
[22] M K Sharma, R K Gupta and W Scheid, *J. Phys. G: Nucl. Part. Phys.* **26**, L45 (2000)
[23] S Singh and R K Gupta, *DAE Nucl. Phys. Symp.* (1993); *Int. Conf. Nucl. Data for Sc. and Tech. Gatlinburg, Tenn., USA* (1994)